Jens Reimann*, Marco Schwerdt, Kersten Schmidt, Nuria Tous Ramon and Björn Döring

The DLR Spaceborne SAR Calibration Center

DOI 10.1515/freq-2016-0274
Received September 19, 2016

Abstract: A necessary activity for any SAR system is its calibration to establish the relation between radar measurements and geophysical parameters. During this process, all essential parameters of a SAR image are linked to their geophysical quantities. This includes the geolocation of the SAR image, its backscattering characteristics (in amplitude and in phase) and polarimetric information. The Microwaves and Radar Institute of the DLR has gained extensive experience in these calibration procedures during the last decades and has developed special methods and dedicated reference targets for spaceborne SAR system calibration. Through examples of calibration results obtained for different spaceborne SAR mission, the capabilities of the DLR SAR Calibration Center are presented.

Keywords: SAR calibration, transponder, corner reflector, Sentinel-1, TerraSAR-X

1 Introduction

In order to keep up with the growing demand for accurate SAR data products on the one hand and the growing complexity of innovative spaceborne SAR system on the other (with a multitude of different imaging beams and novel operation modes like TOPS (Terrain Observation by Progressive Scans, [1]), sliding spotlight, etc.), sophisticated concepts, precise algorithms, and adequate facilities are required to efficiently calibrate such complex spaceborne SAR systems.

Novel concepts and methods along the innovative algorithms have been developed and implemented in a number of tools for analyzing and evaluating the various SAR measurements. The resulting calibration parameters are then used to generate accurate SAR data products.

***Corresponding author: Jens Reimann,** Institut für Hochfrequenztechnik und Radarsysteme, Deutsches Zentrum für Luft- und Raumfahrt e.V., 82234 Wessling, Germany,
E-mail: jens.reimann@dlr.de
http://orcid.org/0000-0002-0650-9073
Marco Schwerdt, Kersten Schmidt, Nuria Tous Ramon, Björn Döring, Institut für Hochfrequenztechnik und Radarsysteme, Deutsches Zentrum für Luft- und Raumfahrt e.V., 82234 Wessling, Germany

In this paper, we present the achievable state-of-the-art calibration accuracy using results from different spaceborne SAR missions, such as TerraSAR-X [2], TanDEM-X [3] and Sentinel-1A [4]. DLR's Microwaves and Radar Institute has been an active player in SAR system calibration since the launch of the first European SAR satellite ERS-1 and has accumulated more than 25 years of experience in this field [5].

2 Challenges and strategy

An efficient calibration strategy has to be individually developed for each and every SAR mission to satisfy its specific requirements and to ensure a product release as soon as possible at the end of the satellite's in-orbit commissioning phase. A general, proven concept [6], which is frequently applied is based on the use of an antenna model to predict the performance of the active phased SAR array antenna and its hundreds of beams.

The SAR system calibration (Figure 1) includes the following activities:

1. Internal Calibration, to guarantee a stable instrument,
2. Geometric Calibration, to to estimate and correct for any SAR system timing bias to enable an accurate image geolocation.
3. Antenna Pointing Determination, to obtain a well-known antenna beam pointing.
4. Antenna Model Verification, to ensure the provision of precise reference patterns (including the gain offset between different SAR beams and sub-swaths) required for all operation modes.
5. Absolute Radiometric Calibration, for radiometric bias correction of SAR data products.
6. Polarimetric Calibration, for correcting polarimetric distortions.

3 DLR SAR calibration facility

The DLR SAR Calibration Facility is a well-equipped center for the calibration of spaceborne SAR systems. An important element is the infrastructure required for the preparation and execution of calibration campaigns

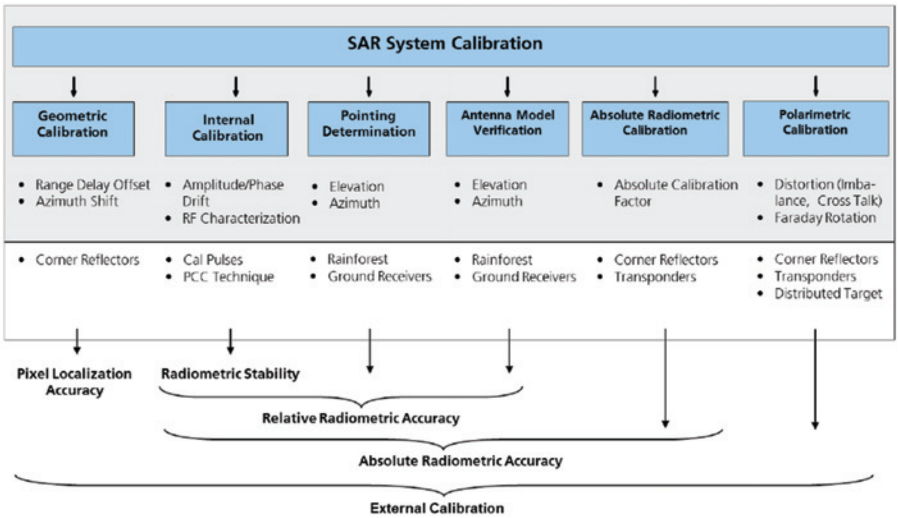

Figure 1: SAR system calibration procedures required for achieving absolute radiometric and geometric calibration of SAR data products.

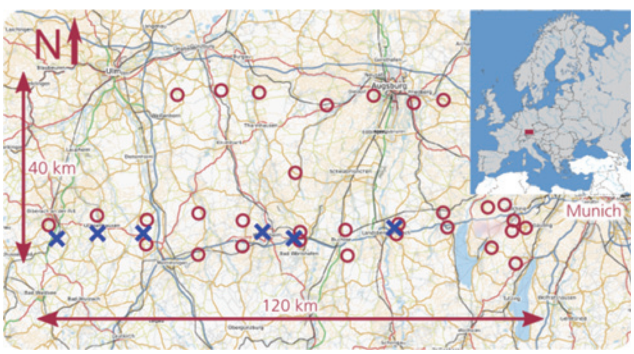

Figure 2: The DLR calibration field consists of 36 target positions with 20 permanently installed corner reflectors. The newly installed six remotely controlled targets are marked by blue crosses. (Map: OpenStreetMap contributers, Overview: David Liuzzo, CC-BY-SA-2.0-de).

Leg Length	2.8m
Radar Cross Section, RCS (X-,C-,L-Band)	54.26, 49.23, 36.56 dBm^2
Mechanical Tolerance	$\leq$ 1.0 mm
Abs. Radiometric Accuracy	0.2 dB (1σ)
Pointing Accuracy	$<$0.1 deg

Figure 3: The new remotely controlled corner reflector.

using extended test sites. The Institute has developed and built a multitude of active and passive calibration targets and operates and maintains a large calibration site in Southern Germany (Figure 2). In 2014 six new sites have been established for the calibration of ESA's Sentinel-1A mission. Three of them were equipped with new precise, remotely controlled trihedral corner reflectors (Figure 3). On the other three sites, the novel in-house developed C-band radar transponders named Kalibri have been deployed (Figure 4).

A radar transponder is an active on-ground device which receives the radar signal transmitted by the satellite, optionally modifies it (e. g. amplification), and finally re-transmits it. For calibration purposes, transponders with high amplification gain are used to improve the Signal-to-Clutter Ratio (SCR) in comparison to passive calibration devices, such as corner reflectors. Transponders can be built to produce different polarimetric signatures. Furthermore transponders can be used to operate as ground receivers recording signals transmitted by the SAR satellite during an overpass. Amongst others these data can be used to retrieve the 1-way azimuth pattern of the SAR antenna and to analyze the shape of individual radar pulses.

The novel in-house developed C-band transponder "Kalibri" is based on a two-antenna design which ensures that there is only a very small time delay between receiption and re-transmission of the radar signal. In addition, it provides a large Radar Cross Sections (RCS) due to reduced back coupling. All transponder

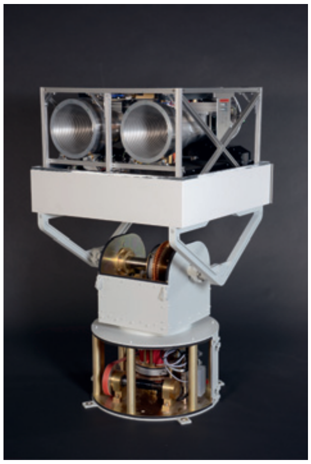

Center Frequency	5.405 GHz
Bandwidth	100 MHz
Radar Cross Section, RCS	60 dBm^2
Radiometric Stability	$\leq$ 0.1 dB (1σ)
Abs. Radiometric Accuracy	0.2 dB (1σ)
Polarization	flexible backscatter matrix

Figure 4: The DLR C-band remotely controlled transponder named Kalibri.

electronics including the antennas are placed inside a water-proof housing. In combination with a precise temperature regulation within the box, this modern design provides very stable RCS values. The transponder electronics are split into widely independent modules: the temperature control, the digital data handling and recording, and the radio frequency parts which operate autonomously and can be individually replaced. This does not only simplify maintenance, but also enables an easy adaption to other frequency bands, such as X-band, which was likewise developed.

Besides the calibration hardware, the DLR SAR Calibration Center also develops SAR data analysis tools to support calibration: For example, several data analysis and calibration tools have been developed to derive calibration parameters from measurements performed during the in-orbit commissioning and the nominal operation of the satellite SAR system like TerraSAR-X, TanDEM-X, PAZ, ALOS, Sentinel-1.

4 Internal calibration

In addition, an innovative Pulse Coded Calibration technique (PCC) has been developed [7], which enables that the nominal calibration pulses generated within the SAR instrument are used for instrument drift monitoring and correction of the SAR raw data in the SAR processor. The PCC technique can be applied to monitor and characterize the antenna's individual transmit-receive-modules (TRMs). This technique, also known as the PN-gating method, was successfully verified in-flight by TerraSAR-X and then applied to TanDEM-X and Sentinel-1A [6]. This technique allows for the monitoring of the gain and phase of each individual TR module for the transmit (TX) and receive path (RX). The resulting values are compared with module specific reference value (i. e. gain and phase); the deviations are regularly monitored over time to detect possible drifts and module degradations.

The deviation of each individual TR module has been measured for TerraSAR-X and TanDEM-X and the results for both satellites are shown for gain (Figure 5) and phase (Figure 6); red lines and black error bars indicate the mean value and standard deviation for each module, respectively. For both satellites, the gain in the transmit path is very stable, whilst in the receive path there is a gain variation depending on the specific behavior of the TR modules, which is however still within the specification of 0.3 dB (1σ). Regarding phase deviations, no TR module degradation is detectable for either satellite.

The standard deviations of all modules are averaged to get an overview of the stability of the SAR instrument i. e. gain and phase during in-orbit operations. The results are summarized in Table 1 and show a very stable instrument in both systems since launch (TerraSAR-X: 2007, TanDEM-X: 2010). Hence, the PCC technique allows for the measurement the actual settings of individual TRMs down to an accuracy of one tenth of a dB in amplitude and one degree in phase.

5 Geometric calibration

The geometric calibration is the estimation of systematic SAR timing offsets in range and azimuth by measuring the the Range-Doppler geolocation of known reference targets in a SAR image. For geometric calibration, the position for both the satellite and the reference target on the ground need to be precisely known. The major effects that can cause a range delay of the radar signal are as follows:

- the internal electronic delay of the instrument and
- atmospheric path delay of ionosphere and troposphere.

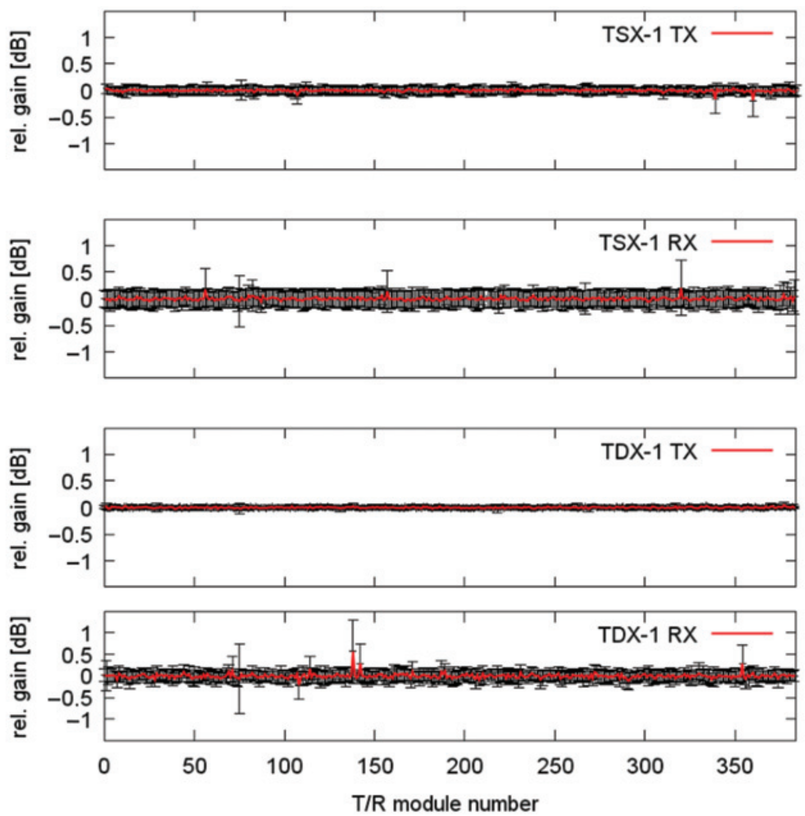

Figure 5: TRM gain deviation over the life time of TerraSAR-X and TanDEM-X since launch separated by receive (RX) and transmit (TX) path.

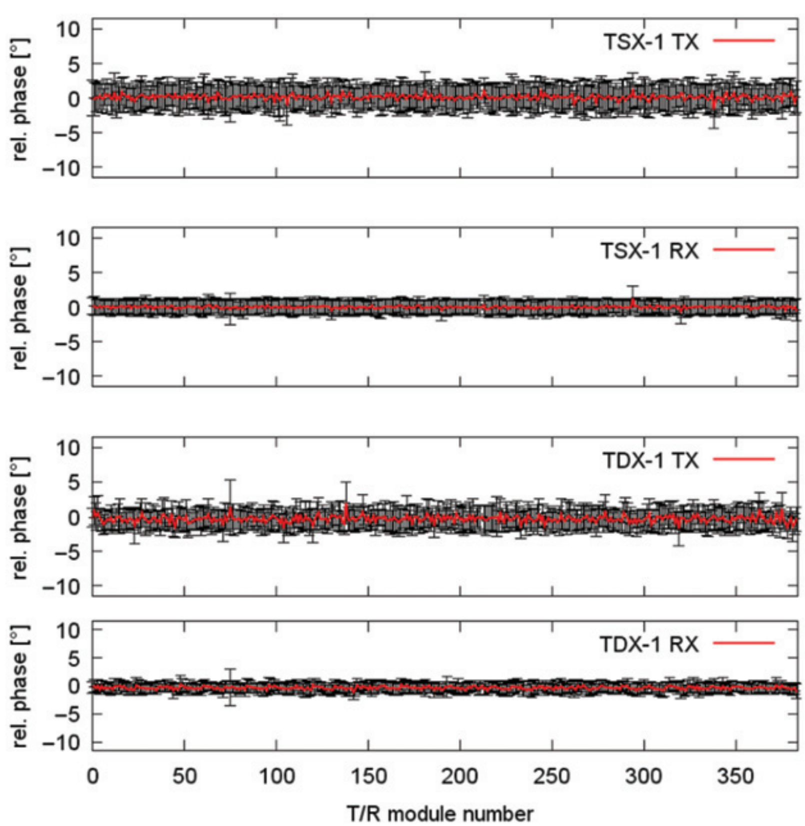

Figure 6: TRM phase deviation over the life time of TerraSAR-X and TanDEM-X since launch separated by receive and transmit path.

Table 1: Statistics of gain and phase T/R-module deviations for transmit and receive path for TerraSAR-X and TanDEM-X satellites.

Mean over the σ-values of all modules	TX		RX	
	Gain [dB]	Phase [deg]	Gain [dB]	Phase [deg]
TerraSAR-X	0.08	2.04	0.17	1.15
TanDEM-X	0.03	1.72	0.15	1.02

While the effect of the ionosphere is negligible for high frequencies, the impact of the troposphere has to be considered. The additional (one-way) correction due to the troposphere is calculated according to [8] and [9] by taken into account the zenith path delay (ZPD, see eq. (1)), the incidence angle (θ), the altitude of the point target (h), and a scaling height (h_s) which is set to 8 km, a typical upper cloud border in the midlatitudes.

$$\Delta r_{tropo} = ZPD \cdot e^{-h/h_s} \cdot \frac{1}{cos\ \theta} \tag{1}$$

In case of TerraSAR-X and TanDEM-X a pixel localization accuracy on the order of 10 cm was achieved [10]. This accuracy is about one order of magnitude better than the requirement of 1 m. With this accurately calibrated TerraSAR-X system, the impact of propagation effects on the range delay could be for the first time verified by a SAR system, as shown in Figure 7. The theoretical path extension caused by tropospheric refraction along the hydrostatic path, which is well known from the global positioning system (GPS), is depicted by the pink line.

If we furthermore compare the range delay offset of TerraSAR-X and TanDEM-X systems, i. e. concentrating on the mean value of the measurements for the respective satellite, the retrieved range delay of both systems differs by only approximately 54 psec. This means, the geometric offset between both satellites in a distance of about 600 km is only 8 mm and this is only one quarter of the wavelength. Hence, the user of SAR data products will not be able to geometrically distinguish whether the SAR image was acquired by the TerraSAR-X or by the TanDEM-X satellite.

6 In-flight antenna characterization

The actual SAR antenna pointing needs to be preciously known to ensure the correct illumination of the scene and to precisely perform antenna pattern correction during SAR data processing. The calibration estimates the difference between the real antenna pointing and the commanded pointing direction. This can be efficiently measured by using so-called notch beams in elevation or in azimuth, which are dedicated SAR beams with a gain drop in the boresight direction. Based on these notch patterns, the boresight direction can be precisely recognized, i. e. in elevation using rainforest scenes or in azimuth by transponder measurements. For TerraSAR-X and TanDEM-X the pointing knowledge was proven to be better than 0.002 deg in both azimuth and elevation [10]. Hence, by readjusting the attitude of the satellite, the detected mispointing of the antenna beam can be precisely removed.

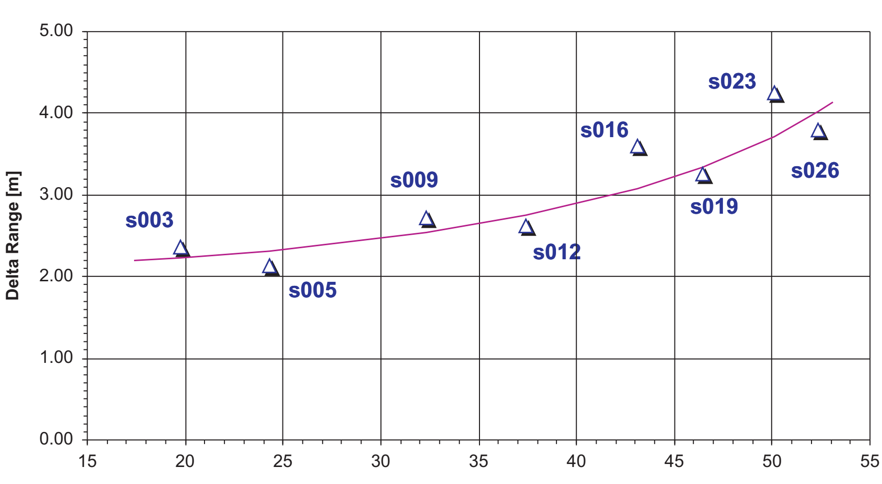

Figure 7: Range offset derived from the range delay and measured for different beams of TerraSAR-X (triangles). The theoretical path extension by hydrostatic effects is depicted by the pink line.

The key element for an efficient radiometric calibration is a precise antenna model. This allow that most of the antenna in-orbit characterization of the SAR antenna, such as verification of the antenna pattern can be shifted from the commissioning phase to pre-launch activities. In particular, the antenna model provides not only the shape of the patterns (as required for the radiometric correction across the scene) but also the gain offsets between different beams and sub-swatch (i. e. in the case of ScanSAR and TOPS). Thus, absolute radiometric calibration can rely on one absolute calibration factor valid for all beams and SAR modes. However, a suitable set of beams has to be measured in-flight to verify the antenna model. For this purpose the Institute has derived several specific methods and procedures [11].

The antenna one-way pattern in azimuth can be recorded by transponders. Due to the movement of the satellite, an azimuthal cut through the pattern is seen by the transponder. For Sentinel-1A, the accuracy of the antenna model was verified to be better than 0.1 dB within the 3 dB beamwidth (Figure 8) [12].

The long-term statistics of the antenna patterns measured since the launch of TerraSAR-X and TanDEM-X (using Amazon rainforest scenes) are shown in Figure 9. TerraSAR-X (TSX-1) datatakes are displayed in blue, TanDEM-X (TDX-1) in green. The mean values have been shifted to zero to focus on relative deviations between the measured and the calculated set of patterns (Note: absolute calibration is preformed against accurate reference targets with well-known RCS, see section 7). The minimum and maximum deviations (4 beams in ScanSAR mode) are represented by an error bar per acquisition. The standard deviations are depicted by triangles. It can be seen in Figure 9 that the behaviour of antenna pattern is very stable over a time period of nearly 7 years. While the standard deviations are always within a limit of ± 0.2 dB, the extreme values do not

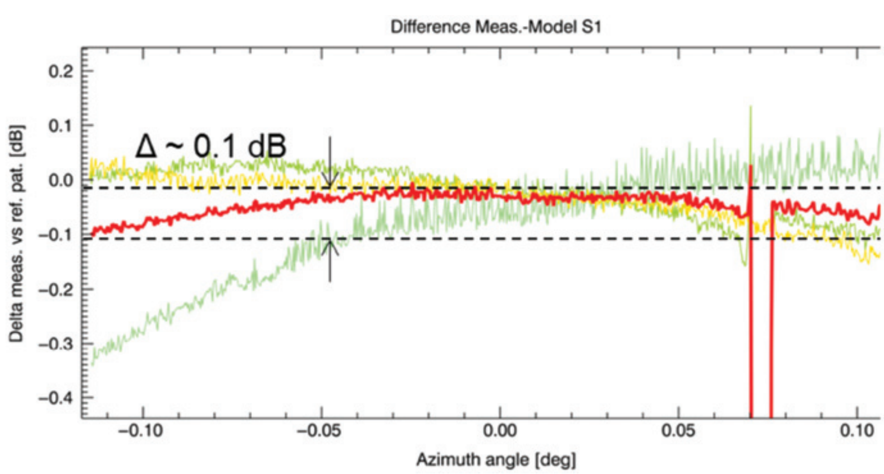

Figure 8: Relative difference between the azimuth antenna pattern measured by the DLR transponders (in yellow and green) and derived by the antenna model within the 3 dB beam width. The mean of all transponder measurements is shown in red.

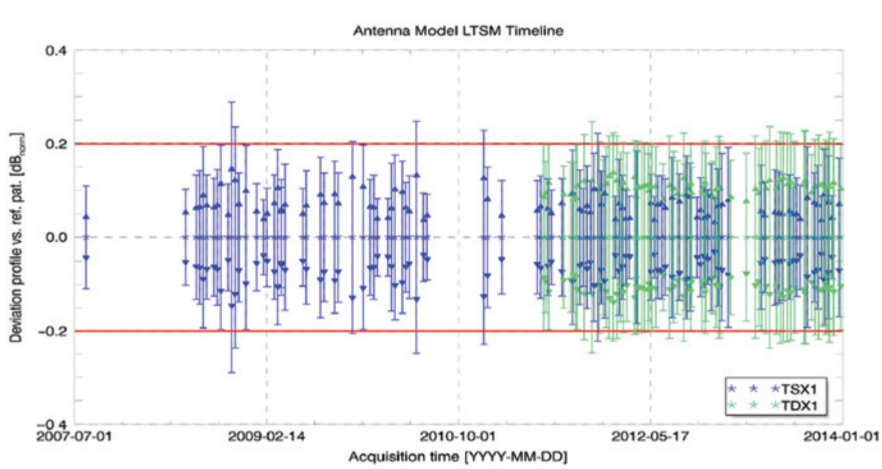

Figure 9: Time series of antenna pattern statistics derived from distributed target scenes (Amazon rainforest) by operating the instrument in ScanSAR mode for TSX-1 (blue) and TDX-1 (green).

exceed ± 0.3 dB. The statistics show that there is no noticeable difference in the radiometric performance between both satellites.

Analyzing the whole azimuth antenna pattern becomes a real challenge for the TOPS modes as utilized by the Sentinel-1 mission due to the sophisticated antenna beam steering in azimuth (up to 5 sub-swathes each steered by more than 800 azimuth beams, see Figure 10). Nevertheless, DLR was able to verify this complicated one-way antenna pattern in TOPS operation [13].

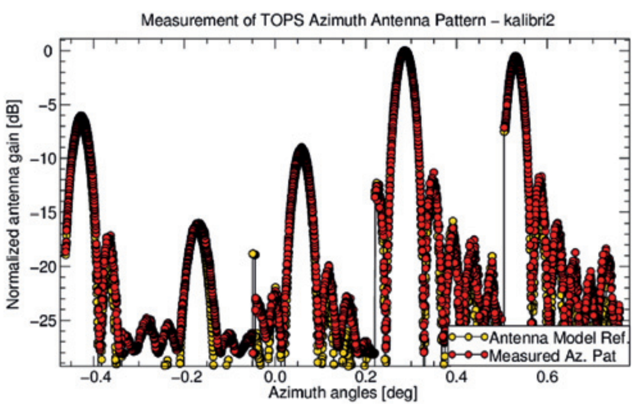

Figure 10: Comparison of the very complicated azimuth pattern in TOPS operation (EW mode) between antenna model (orange) and transponder measurements (red).

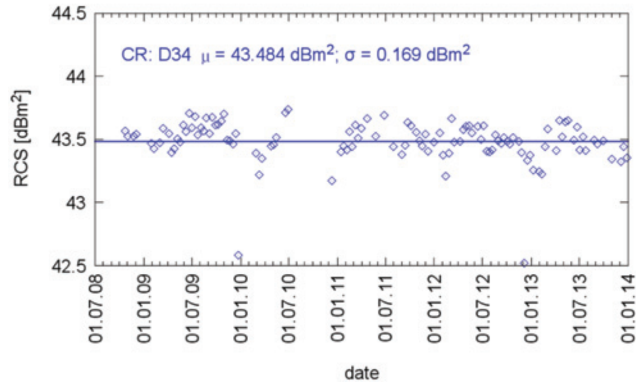

Figure 11: Time series of radar cross section (RCS) derived from permanently installed corner reflectors for TSX-1.

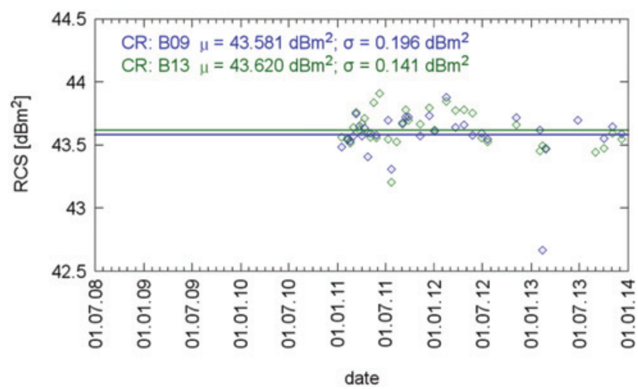

Figure 12: Time series of radar cross section (RCS) derived from permanently installed corner reflectors for TDX-1.

7 Absolute radiometric calibration

As a final step of the radiometric radiometric calibration the entire SAR system is end-to-end measured against reference targets with well-known RCS [14], [15]. In particular, as the shape of the antenna pattern and the gain-offset between different beams have already been compensated for by applying the antenna model during SAR data processing, the absolute calibration factor is independent of both the target position within the swath and the SAR beam mode.

In fact, as depicted in Figures 11 and 12, the RCS values derived from TanDEM-X measurements of the reference targets have an equal distribution without any significant trend [16]. Consequently, the absolute radiometric accuracy is derived from the standard deviation of all measurements. For TanDEM-X we have achieved an absolute radiometric accuracy of 0.14 dB for the StripMap mode during the commissioning phase. Additionally, considering the same radiometric stability (0.15 dB as derived for TerraSAR-X two years after launch by an comprehensive recalibration campaign executed in 2009 [6]) and propagation uncertainties of 0.25 dB, an absolute radiometric accuracy of less than 0.5 dB could be achieved for TanDEM-X [17].

8 Polarimetric calibration

Polarimetric calibration analyses and corrects perturbation in polarimetric SAR images. There are two main objectives: adjustment of all polarimetric channels and estimation of the cross talk between channels. To achieve both objectives, the Faraday rotation along the propagation path has to be estimated.

According to [18] and neglecting noise contributions the measured scattering properties M of a target can be modeled as:

$$M = A(r,\theta)e^{j\phi}\begin{bmatrix}1 & \delta_2\\ \delta_1 & 1\end{bmatrix}\begin{bmatrix}1 & 0\\ 0 & f_1\end{bmatrix}\begin{bmatrix}\cos\Omega & \sin\Omega\\ -\sin\Omega & \cos\Omega\end{bmatrix}\begin{bmatrix}S_{hh} & S_{vh}\\ S_{hv} & S_{vv}\end{bmatrix}\begin{bmatrix}\cos\Omega & \sin\Omega\\ -\sin\Omega & \cos\Omega\end{bmatrix}\begin{bmatrix}1 & 0\\ 0 & f_2\end{bmatrix}\begin{bmatrix}1 & \delta_3\\ \delta_4 & 1\end{bmatrix} \quad (2)$$

where δ_1, δ_2, δ_3, and δ_4 are depolarization terms, f_1 and f_2 are channel imbalances, Ω is the Faraday rotation angle, $A(r,\theta)$ the range and angle dependent path attenuation, ϕ the absolute phase, and S_{hh}, S_{vh}, S_{hv}, and S_{vv} the scattering coefficients of the targets.

By analyzing targets with known scattering matrix within a scene the unknown parameters in eq. (2) can be estimated. Trihedral corner reflectors are especially suited to retrieve the cross polarization level as they do not depolarize an incident wave. Transponders, as those shown in Section 3, can synthesize various scattering matrices and are therefore very suitable to realize the scattering coefficients of eq. (2) within a SAR scene. Furthermore by means of a ground receiver unit they are also well suitable to measure the one-way cross polarization level of the SAR instrument on transmit.

Figure 13 shows the absolute calibration factors for the four polarimetric channels of TerraSAR-X in Dual Receive Antenna (DRA) mode as measured during a recalibration campaign in 2009. After introducing a slight offset of –0.18 dB for the antenna gain of all V polarization patterns on receive, a maximal channel imbalance between all polarization channels of 0.26 dB has been achieved [19].

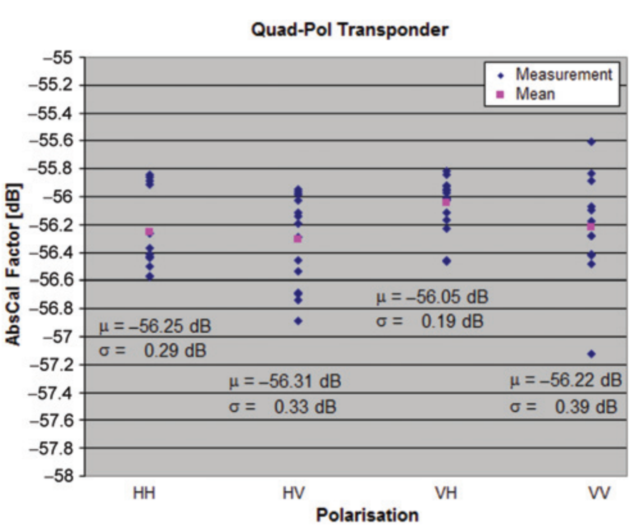

Figure 13: Absolute radiometric calibration factor for the four polarimetric channels of TerraSAR-X in DRA mode [19].

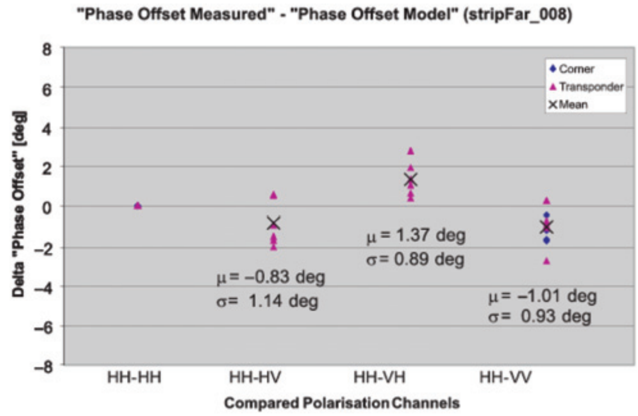

Figure 14: Residual polarimetric phase of TerraSAR-X in DRA mode after compensating the phase derived from the antenna model [19].

The relative phases (referenced to channel HH) between the polarimetric channels are presented in Figure 14. Compensating the phase characteristic of the antenna by introducing phase patterns derived from the antenna model, a residual phase imbalance of less than 2.2 deg could be achieved [19].

9 Conclusion

Calibration of spaceborne SAR systems is a traditional R&D field in the DLR Microwaves and Radar Institute. During the last 20 years, not only has the demand for highly accurate spaceborne SAR data products increased but also the level of complexity in the SAR instrument architecture and the instrument's built-in calibration system. To keep pace with this development, the Microwaves and Radar Institute has built up, maintained and extended the DLR SAR Calibration Center, including innovative targets like remotely controlled trihedral corner reflectors and the in-house developed C-band transponders "Kalibri", as well as novel tools for product quality control and performance analysis.

Through examples of different spaceborne SAR systems, important aspects of SAR system calibration were described (including internal calibration, geometric calibration, antenna pointing determination, antenna model verification, and absolute radiometric calibration) and the accuracy of the different calibration techniques/methods were shown, as summarized in Table 2.

Table 2: DLR calibration methods and achieved accuracies.

Estimation of (monitored) Instrument Drift: Amplitude /Phase	< 0.1 dB /< 1 deg
TRM Characterization (PCC): Amplitude /Phase setting	< 0.2 dB /< 2 deg
Geometric Calibration: Azimuth /Range	~10 cm /~10 cm
Pointing Determination: Azimuth /Elevation	< 2 mdeg /< 2 mdeg
In-orbit Antenna Model: Verification	< ± 0.2 dB
Channel Imbalance: Amplitude /Phase	< 0.4 dB /< 3 deg
Radiometric Calibration	
Accuracy	< 0.3 dB
Stability	< 0.2 dB

References

[1] F. D. Zan and A. M. Guarnieri, “TOPSAR: Terrain obsercation by progressive scans,” *IEEE Trans. Geosci. Remote Sens.*, vol. 48, no. 2, pp. 2352–2360, 2010.

[2] M. Schwerdt, B. Bräutigam, M. Bachmann, B. Döring, D. Schrank, and J. H. Gonzalez, “Final results of the efficient TerraSAR-X calibration method,” in *2008 IEEE Radar Confrerence*, Rome, Italy, 2008.

[3] J. H. Gonzalez, B. Bräutigam, M. Schwerdt, and M. Bachmann, “Terrasar-x internal calibration experience and extension for tandem-x,” in *Proceedings of CEOS SAR Cal/Val Workshop* 2008 Oberpfaffenhofen, *Germany*, 2008.

[4] M. Schwerdt, K. Schmidt, N. T. Ramon, G. C. Alfonzo, B. Döring, M. Zink, and P. Prats, “Independent verification of the Sentinel-1A system calibration - first results,” in *10th European Conference on Synthetic Aperture Radar*, Berlin, Germany, 2014.

[5] J. Reimann, M. Schwerdt, K. Schmidt, N. T. Ramon, G. A. Castellanos, B. Dãring, D. Rudolf, S. Raab, J. M. W. Antony, and M. Zink, “The DLR SAR calibration center,” in *2015 IEEE 5th Asia-Pacific Conference on Synthetic Aperture Radar (APSAR)*, Sept. 2015, pp. 169–173.

[6] M. Schwerdt, B. Bräutigam, M. Bachmann, B. Döring, D. Schrank, and J. H. Gonzalez, “Final TerraSAR-X calibration results based on novel efficient methods,” *IEEE Trans. Geosci. Remote Sens.*, vol. 48, no. 2, pp. 677–689, 2010.

[7] D. Hounam, M. Schwerdt, and M. Zink, “Active antenna module characterisation by pseudo-noise gating,” in *25th ESA Antenna Workshop on Satellite Antenna Technology*, Noordwijk, Netherlands, 2002.

[8] M. Jehle, D. Perler, D. Small, A. Schubert, and E. Meier, “Estimation of atmospheric path delays in TerraSAR-X data using models vs. measurements,” *Sensors*, vol. 8, no. 12, pp. 8479–8491, 2008.

[9] O. Frey, E. Meier, D. Nüesch, and A. Roth, “Geometric error budget analysis for TerraSAR-X,” in *5th European Conference on Synthetic Aperture Radar EUSAR*, 2004, pp. 513–516.

[10] M. Schwerdt, D. Schrank, M. Bachmann, J. H. Gonzalez, B. Döring, N. Tous-Ramon, and J. W. Antony, “Calibration of the TerraSAR-X and the TanDEM-X satellite for the TerraSAR-X mission,” in *9th European Conference on Synthetic Aperture Radar*, 2012.

[11] M. Schwerdt, B. Döring, M. Zink, and D. Schrank, “In-orbit calibration plan for Sentinel-1,” in *8th European Conference on Synthetic Aperture Radar*, 2010.

[12] M. Schwerdt, K. Schmidt, N. T. Ramon, G. C. Alfonzo, B. J. Dãring, M. Zink, and P. Prats-Iraola, “Independent verification of the Sentinel-1a system calibration,” *IEEE J. Sel. Top. Appl. Earth Obs. Remote Sens.*, vol. 9, no. 3, pp. 994–1007, Mar. 2016.

[13] G. C. Alfonzo, M. Schwerdt, B. Döring, N. T. Ramon, and K. Schmidt, “First results of the Sentinel-1A in-orbit antenna characterization performed by DLR,” in *10th European Conference on Synthetic Aperture Radar*, 2014.

[14] B. J. Döring, M. Jirousek, D. Rudolf, S. Raab, J. Reimann, and M. Schwerdt, “The three-transponder method: A novel method for accurate transponder RCS calibration,” *Prog. Electromagn. Res. (B)*., vol. 61, pp. 297–315, 2015.

[15] B. J. Döring, K. Schmidt, M. Jirousek, R. Daniel, J. Reimann, S. Raab, A. John, and M. Schwerdt, “Hierarchical Bayesian data analysis in radiometric sar system calibration: A case study on transponder calibration with RADARSAT-2 data,” *Remote Sens.*, vol. 5, no. 12, pp. 6667–6690, 2013.

[16] K. Schmidt, G. C. Alfonzo, N. T. Ramon, M. Bachmann, and M. Schwerdt, “Calibration performance of the TerraSAR-X and TanDEM-X satellites since launch,” in *10th European Conference on Synthetic Aperture Radar*, 2014.

[17] M. Schwerdt, J. H. Gonzalez, M. Bachmann, D. Schrank, B. Döring, N. T. Ramon, and J. M. W. Antony, “In-orbit calibration of the TanDEM-X System,” in *30th International Geoscience*
And Remote Sensing Symposium, Vancouver, Canada, 2011.

[18] A. Freeman, “Calibration of linearly polarized polarimetric SAR data subject to Faraday rotation,” *IEEE Trans. Geosci. Remote Sens.*, vol. 42, pp. 8, 2004.

[19] M. Schwerdt, D. Schrank, M. Bachmann, C. Schulz, B. Döring, and J. H. Gonzales, “TerraSAR-X re-calibration and dual receive antenna performed in 2009,” in *8th European Conference on Synthetic Aperture Radar*, Aachen, Germany, 2010.